Study of copper–alumina bonding

C. BERAUD*, M. COURBIERE‡, C. ESNOUF*, D. JUVE‡, D. TREHEUX‡
*Institut National des Sciences Appliquées, GEMPPM, Bât. 502,
20 Avenue Albert Einstein, 69621 Villeurbanne cédex, France
‡Ecole Centrale de Lyon, Laboratoire de Métallurgie,
36 Avenue Guy de Collongues, 69131 Ecully cédex, France

Bonding between copper and alumina can be obtained by the "solid state bonding" process and the "liquid phase bonding" process. The strength of interfaces has been tested mechanically using shear tests, tensile tests and fracture toughness tests. The effects of bonding parameters on bond strength have been studied. Observations by transmisssion electron microscopy have been performed to detect and analyse the nature and evolution of interfacial compounds as a function of copper oxidation and bonding time. Chemical reactions lead to the formation of the binary oxide $CuAlO_2$. The stability of this compound and the reversibility of chemical reactions appear to be very dependent on the amount of oxygen present in the system.

1. Introduction

The applications offered by the association of ceramics and metallic materials have been generating a great deal of interest for several years. Especially the use of ceramics as a protective coating on a metal surface in corrosive atmospheres or at high temperature extends the field of industrial applications when materials with optimal characteristics are required. Such a context explains the development of metal to ceramic joining techniques in order to obtain reliable bonds. The feature of these "composite" materials consists of the coupling of very different properties; the physical and chemical phenomena involved during the bonding process are complex and not well understood yet. Many studies have been carried out on different metal–ceramic couples; two types of bonds can be distinguished:

1. Bonds performed in a reducing atmosphere preventing the formation of an interfacial compound.

2. Bonds performed in a non-reducing atmosphere leading to the formation of an interfacial compound.

Klomp [1, 2] has studied solid state bonds between alumina and both noble or transition metals. Using a reducing atmosphere of hydrogen, the formation of oxides is strictly avoided. The author suggests that in this case, evaporation–condensation phenomena and surface diffusion of metallic atoms lead to the establishment of the bond.

More recently, studies concerning the crystallographic orientation of interfaces have been carried out on different metal–alumina couples [3, 4]. Interesting results are brought up: a preferential crystallographic relationship exists between cubic metals (copper, platinum, niobium) and monocrystalline alumina. A faceting phenomenon is observed at the interface $Nb–Al_2O_3$ [4], this observation can be described in terms of best coincidence between the two lattices where the close packed planes are nearly parallel, however the interpretation of such result is difficult.

Oxygen plays an important role in promoting reliable bonds between metal and ceramic; it may lead to the growth of interfacial oxides as a result of a diffusion process of metallic atoms in the ceramic. Moreover, oxygen being a surface active agent lowers the surface tension of the metal and then enhances the spreading of the liquid and adhesion. O'Brian and Chaklader [5] have studied the effect of oxygen present in copper on the wettability of the alumina substrate by liquid copper: the angle of wettability decreases when the amount of oxygen increases. Similar results are obtained by Eustathopoulos and Passerone [6] using different metals in contact with alumina. Moreover from thermodynamic results, Pask and Tomsia [7] point out the fact that a chemical reaction contributes to a better wettability.

The aim of discussing these previous results was to set the context within which this work was carried out. The atmosphere used during bonding, and especially the amount of oxygen present in the system, has a predominant effect on the nature and properties of the bond.

2. Materials and joining processes

Copper to alumina bonds are performed using two methods: the "solid state bonding" process [8, 9] and the "liquid phase bonding" process [10]. Apparatus and experimental conditions are further described.

2.1. Solid state bonding

During this process several parameters must be controlled:

1. The bonding temperature T_b lies below the melting point of the lowest melting component, that is copper ($T_m = 1083°C$) in our system. T_b is varied from 700 to 1000°C, the heating rate is $5°C\,min^{-1}$;

2. The bonding pressure has to be sufficient to ensure a good contact between the surfaces of the two components; pressure in the range of 1 to 8 MPa are used;

3. The bonding time is varied from 30 min to 6 h;

4. The surface roughness of alumina lies in a range of 0.02 to 1 μm. It is obtained by using different diamond powders, polishing or lapping (soft and hard) and grinding. The surface of copper to be bonded is polished to a finish approaching optical flatness;

5. An argon atmosphere is used during bond formation. The partial pressure of oxygen is 10^{-3} torr, the total pressure of oxygen is 1 atm.

Samples consist of two sections of bulk polycrystalline alumina (99.7% Degussa Al23) connected by a copper foil (Oxygen Free High Conductivity) (OFHC) 0.2 mm thick. Before bonding materials are vacuum annealed (10^{-3} torr) at 1000° C for 30 min. After treatment samples are furnace cooled.

2.2. Liquid phase bonding
This process is based on two facts:

1. An eutectic exists in the copper–oxygen system for a composition of 0.39 wt % of oxygen. The melting temperature of the eutectic (1065° C) lies slightly below the melting temperature of copper (1083° C) [11];

2. The eutectic liquid phase shows good properties concerning the wettability of alumina surfaces; as shown in Fig. 1, a maximum seems to be reached at the eutectic composition [12]. This is in accordance with the fact previously mentioned that the wettability of alumina by liquid copper is strongly increased by the presence of oxygen [5].

In the temperature range of 1065 to 1083° C a liquid phase appears at the Cu_2O–Cu interface, its amount can be controlled by careful regulation of oxide growth on the copper foil. This thin molten film produces an intimate contact between copper and
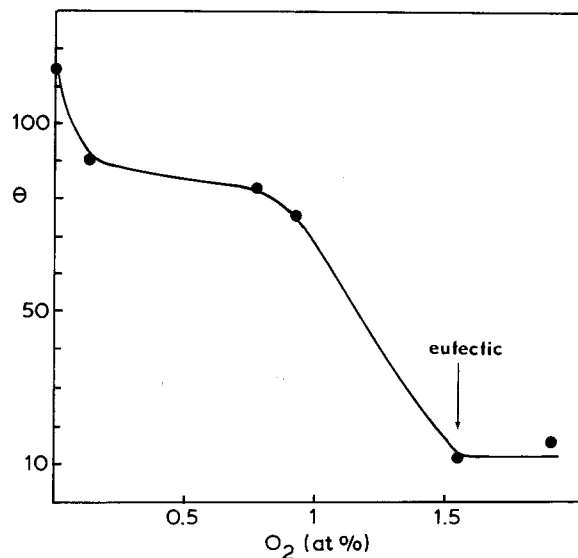
alumina and generates, after cooling, a strong bond between the two materials.

Copper foils (0.2 mm thick) are polished with a 1 μm diamond paste, annealed and then oxidized under low oxygen pressure (10^{-1} torr) at 1000° C giving rise to a superficial adherent Cu_2O film [13]. The thickness of Cu_2O films is varied from 0.3 to 70 μm. The bonding temperature is 1070° C. The bonding time is very short, 2 min. The furnace atmosphere is scanned with argon.

3. Mechanical properties of joints
The strength of interfaces has been measured by a shear test for solid state bonded joints and by a tensile test for liquid phase joints. The test are performed at room temperature with a strain rate of 5 mm min^{-1}. More details are given in a previous work [14].

3.1. Characterization of solid state bonded specimens
3.1.1. Influence of bonding temperature
The effect of temperature on bond strength can be seen in Fig. 2. Bond strength increases with bonding temperature and fractures appear at the copper–alumina interface. The plastic deformation of the copper foil by creep increases with temperature as well, and allows the formation of enlarged contact zones between the two materials (Fig. 3a) during compression. A maximum in contact is reached at 1000° C, the non-adherent areas are located outside of the bond (Fig. 3b).

3.1.2. Influence of bonding pressure
Treatments are performed for 2 h at 1000° C (optimum temperature as previously mentioned). It can be seen from Fig. 4 that the bond strength increases up to a value of 50 MPa for an applied pressure of 3 MPa, then remains approximately constant. The surface of adherent zones can be obtained as a function of the applied pressure (Fig. 5a, b): beyond 4 MPa, intimate contact exists between the copper and alumina surfaces.
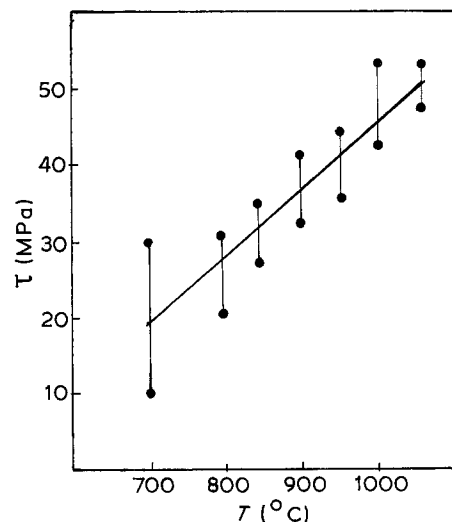

Figure 1 Evolution of contact angle θ for liquid copper upon alumina as a function of oxygen content in the copper drop after cooling [12].

Figure 2 Fracture strength dependence on temperature for solid state bonding (2 h, 6 MPa).
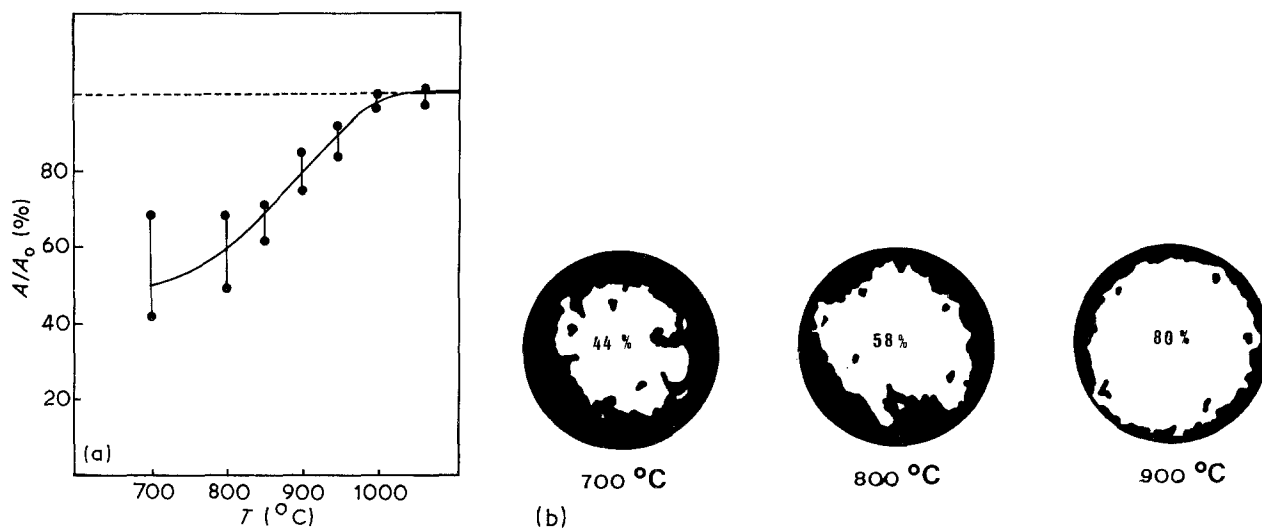
Figure 3 (a) Percentage of adherent zones as a function of temperature (2 h, 6 MPa). (b) Contact areas for different temperatures. Adherent zones are white.

3.1.3. Influence of bonding time

Figure 6 shows the effect of bonding time for two applied pressures: 6 MPa (curve A) and 4 MPa (curve B). For an applied pressure of 6 MPa, no change in bond strength values is recorded with increasing time. For an applied pressure of 4 MPa, the bond strength keeps on increasing beyond the time required to achieve contact between the two surfaces by creep of the metal. From these observations, another mechanism must operate improving the bonding between copper and alumina, as it will be seen further (see section 4.2).

3.1.4. Influence of alumina roughness

Figure 7 shows the variation of the fracture shear strength with alumina roughness. The fracture strength increases with roughness up to about $R_a = 0.5\,\mu m$ when the fracture is located at the ceramic–metal interface, but it falls drastically when the failure occurs in the bulk alumina.

Alumina surfaces before bonding and copper surfaces after failure have been investigated by scanning electron microscopy.
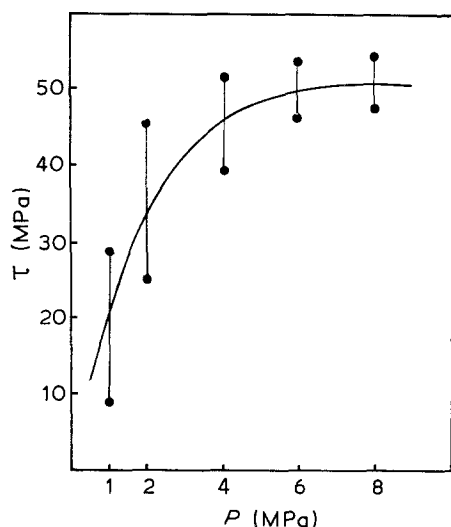

Figure 4 Fracture strength dependence on pressure for solid state bonding (2 h, 1000° C).

1. Concerning the first part of the curve, the sliding lines and ductile cupules observed on copper surfaces (Fig. 8) indicate that the metal is deformed plastically during the formation of the bond. The increase in fracture strength which does not occur for an optical flat alumina surface, can be explained by a better pinning of copper in the residual cavities of the softly lapped alumina. Damage caused on the alumina surface by hard lapping or grinding (pulled out grains and microcracks along grain boundaries) induce a decrease in the fracture strength of the alumina–copper joint.

2. SEM observations after failure show the presence of alumina grains on the copper surface (Fig. 9a, b); this indicates that an intergranular fracture occurs in the first layers of alumina. Though this is not representative of the interface strength, such a behaviour shows that the effect of the alumina surface has to be considered.

3.2. Characterization of liquid phase bonded specimens

3.2.1. Fracture strength of Cu–Al₂O₃ bonds

Tensile test results as a function of the initial Cu_2O thickness are shown in Fig. 10. The optimal strength (140 MPa) is obtained for Cu_2O thickness lying between 3 and 10 μm. Fracture strength, i.e. adhesion, depends on the amount of liquid eutectic and consequently on the Cu_2O layer thickness. In the case of a thin Cu_2O layer ($< 3\,\mu m$), insufficient liquid is formed and only localized adhesion occurs at grain boundaries (Fig. 11). Then, between 3 and 10 μm thickness, the eutectic phase comes into intimate contact with the alumina and rupture occurs at the alumina–eutectic interface or in the eutectic phase. Beyond a Cu_2O thickness of 10 μm, a decrease in tensile strength is observed as a consequence of the numerous large pores (10 to 100 μm) located at the interface (Fig. 12).

3.2.2. Fracture toughness of Cu–Al₂O₃ bonds

The fracture toughness value (K_{Ic} characterizes the resistance to crack initiation (and propagation)
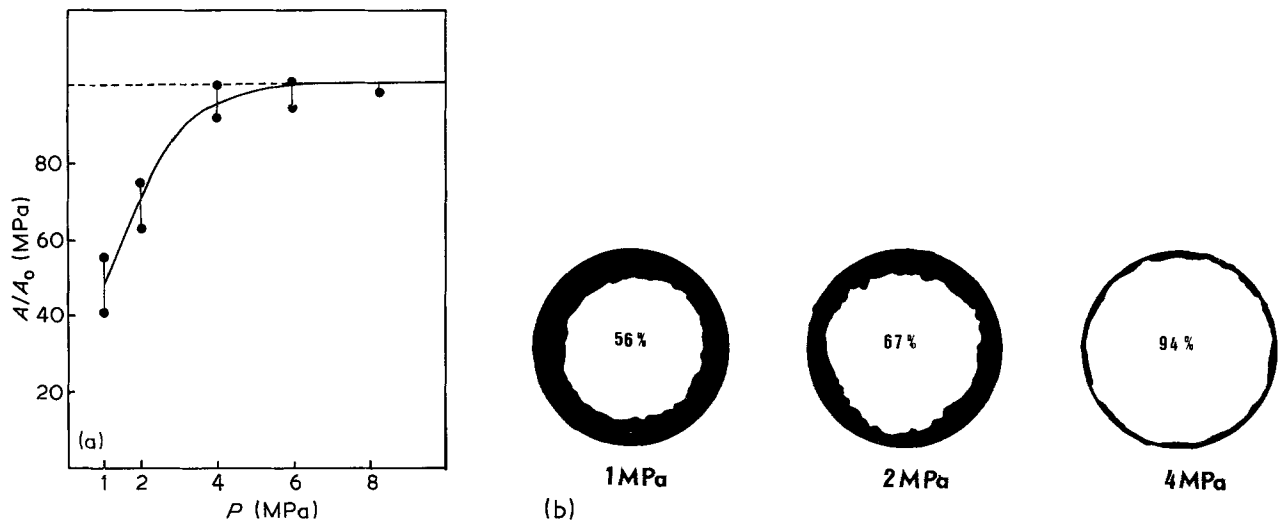
Figure 5 (a) Percentage of adherent zones as a function of applied pressure (2 h, 1000° C). (b) Contact areas for different applied pressure. Adherent zones are white.

of a material. Experimental determination requires the induction of a macroscopic defect of controlled dimensions and the calculation of stress needed to extend this defect. In the case of composite materials made by liquid phase bonding, the determination of the stress needed to propagate a defect localized in the interface can give a good estimation of the bond strength [15].

In our case, fracture toughness tests are performed at room temperature on single edge notched beam specimens, with a four-points bending test (crosshead speed, $0.1 \, mm \, min^{-1}$). Notches have been machined (diamond saw) so as to be located along the interface or within the copper. Results are shown in Fig. 13. The maximum fracture toughness values are in both cases similar to that one of bulk alumina ($3.7 \, MPa \, m^{1/2}$ in the first case: curve A; $4 \, MPa \, m^{1/2}$ in the second case: curve B. Figure 13 is similar to figure 10, the measured K_{Ic} values decrease if the Cu_2O layer is thinner than $3 \, \mu m$ or thicker than $10 \, \mu m$. In the case of the thin Cu_2O layer the fracture energy of the interface is low because insufficient eutectic is formed to wet

all the ceramic surface. With thicker Cu_2O layers, the brittleness of the bond is increased (low toughness values) and the crack resistance behaviour of the interface is considerably reduced compared to that of the bulk alumina.

4. Analysis of mechanisms inducing copper–alumina bonding

4.1. Macroscopic effect

Solid state bonding proceeds primarily by means of the deformation of the metallic foil as a consequence of combined effects of applied pressure and temperature which allows the creation of an intimate contact between the two materials. Nevertheless, this phenomenon is strongly influenced by alumina roughness and the shape and dimensions of the metallic part. Experiments concerning copper creep show that the deformation gets higher when the alumina surface is smoother [12].

The presence of different zones of deformation in the contact area can be explained by a heterogeneous stress distribution in the contact area [14, 15] due to
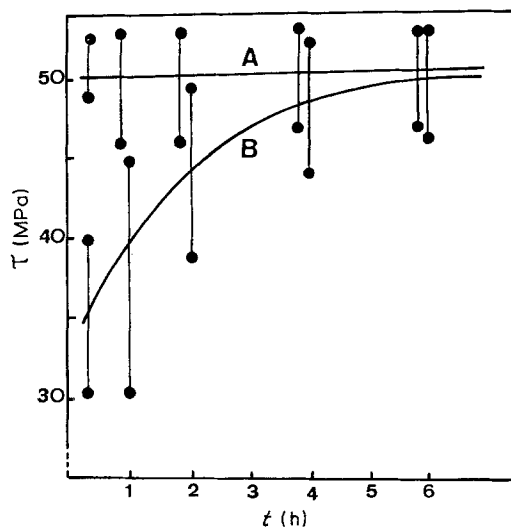

Figure 6 Fracture strength dependence on bonding time (at 1000° C) for solid state bonding. (A) 6 MPa; (B) 4 MPa.
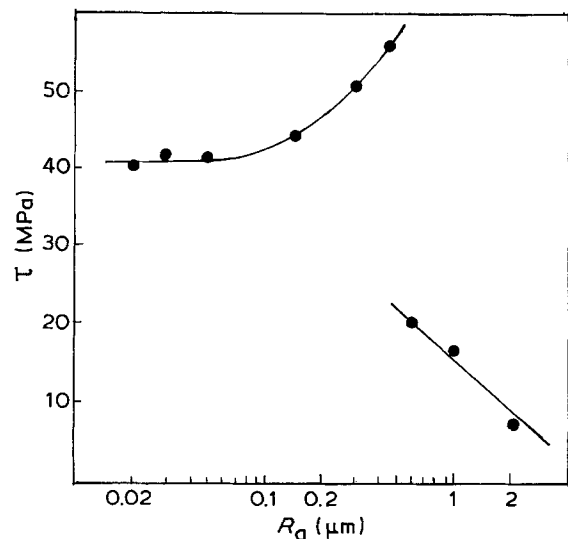

Figure 7 Effect of alumina roughness on fracture shear strength for solid state bonding (2 h, 6 MPa, 1000° C).
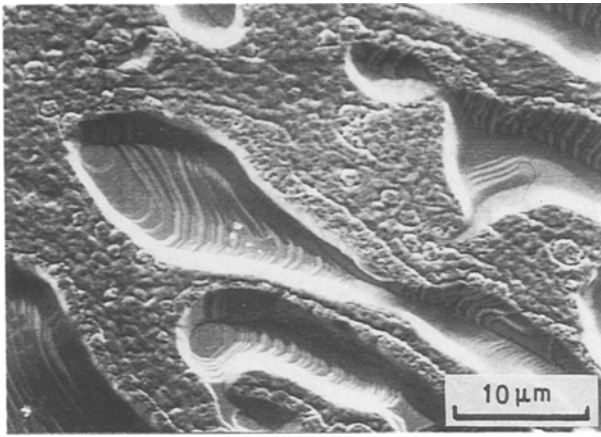
Figure 8 SEM micrograph showing copper surface after failure. Roughness, $R_a = 0.05\,\mu m$; bonding pressure $= 6\,MPa$. Notice the sliding lines present within the cavities. Only few grains of alumina remain in surface.

copper deformation and friction. The shape of the joint characterized by the ratio b/h (length/height) has great importance since the crushing ratio increases with the b/h factor during bonding [12]. When b/h is too high, plastic deformation does not occur [16]. It should be mentioned that this phenomenon is predominant when rings are used as joints instead of metallic foils and when the temperature is raised [17].

The resistance of solid state bonding specimens is concerned with the surface of the contact area, as seen previously (cf Sections 3.1.1. to 3.1.4.). The presence of an unbonded area having a ring shape is propicious to cracks initiation during mechanical tests. Moreover, defects such as pores induced by the gas entrapped at the interface can be observed (Fig. 8) especially when optical flatness and a high b/h ratio are used.

Thus, when the surfaces are macroscopically in contact, according to alumina roughness, metal creeping is not sufficient to fill up the cavities remaining after lapping though they act as anchorage points and contribute to an improvement of the bond as seen earlier (cf Fig. 7).
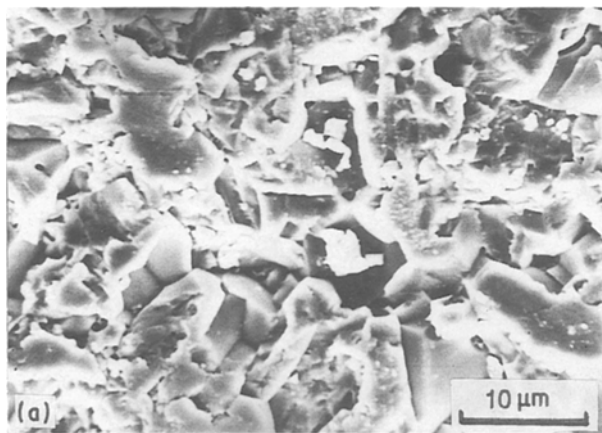
4.2. Microscopic effect

After metal creep has stopped after an enlargement of the contact area, improvement of the bond strength is achieved by increasing the bonding time (Fig. 6). Such a behaviour could be explained by a diffusion process leading to a filling up of the cavities. But a much more interesting approach consists in considering evaporation–condensation phenomena which allow interfacial diffusion. Such an hypothesis is realistic since the copper vapour pressure lies between 10^{-3} and 10^{-4} torr and the time required for a copper monolayer to condense, calculated with the Dushman relation [18], is about 1 sec at 1000° C. This mechanism can dominate in pores and unbonded areas. Bonding achieved by the liquid phase induces a decrease of copper vapour pressure which is liable to expand such a phenomenon.

5. Interfacial reaction between copper and alumina during bonding

The quality of the bond is greatly dependent on the reactions occurring at the interface and consequently on the properties of the resulting products. Given the three elements aluminium, copper and oxygen, compounds are the hexagonal binary oxide $CuAlO_2$ and (or) the cubic spinel phase $CuAl_2O_4$ [19]. Reactions between copper and alumina depend strongly on the reactive atmosphere; oxygen plays an important role in promoting reactions between the two materials in agreement with the equilibrium diagram [19]. Reaction between alumina and copper oxide, CuO, leads to the formation of cubic spinel oxide $CuAl_2O_4$, whereas binary hexagonal oxide, $CuAlO_2$, is obtained when alumina and cuprite oxide react together.

This part of the work is concerned with the effect of superficial oxidation of copper on the growth of interfacial compounds. Superficial oxidation of copper (Cu_2O) is obtained by heating to 1000° C under low oxygen pressure [12].

Observations by TEM are performed on cross sections using a JEOL-200CX transmission electron microscope [20]. These foils are prepared by mechanical polishing and finally by ion bombardment.
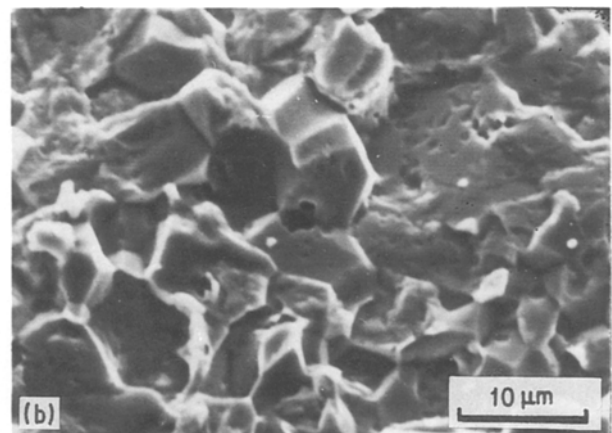

Figure 9 (a) SEM micrograph showing the alumina surface before bonding ($R_a = 2\,\mu m$). It is polished with a 150 μm diamond grinder. (b) SEM micrograph showing copper surface after failure. It is entirely covered with alumina grains pulled out during lapping. Bonding pressure $= 6\,MPa$.
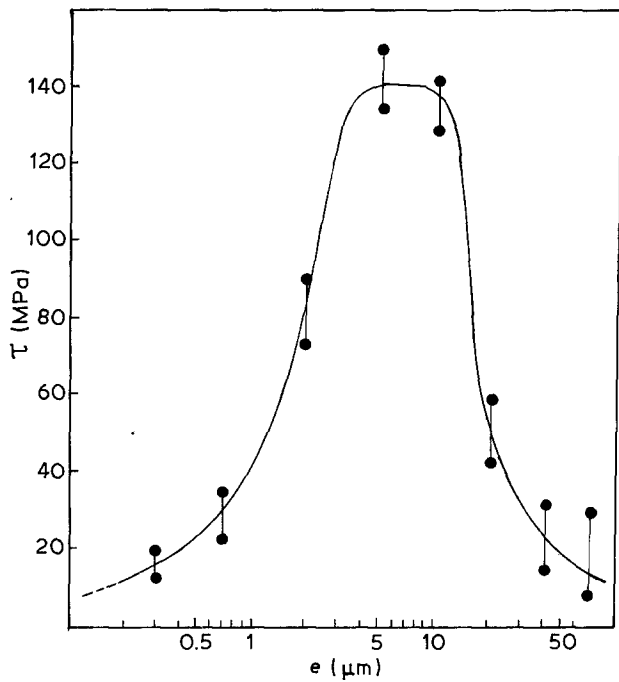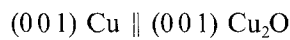
Figure 10 Variations of the tensile strength with initial Cu_2O thickness (1070° C, 2 min) when the eutectic method is used.

5.1. Solid state reactions
5.1.1. Reaction between Cu_2O and Al_2O_3

Superficial oxidation of copper leads to the formation of an initial Cu_2O thickness of 0.7 μm. Treatment for 2 h at 4 MPa at 1000° C, under argon, the binary oxide $CuAlO_2$ (0.2 to 0.4 μm thick) is found to be present at the interface (Fig. 14). The compound $CuAlO_2$ contains many twins in the (0 0 0 1) plane running parallel to the interface [20]. No crystallographic relationship between Cu_2O, Al_2O_3 and $CuAlO_2$ has been found. Copper appears to be enriched with small precipitates of copper oxide Cu_2O in perfect epitaxy with the matrix of copper according to the epitaxial relations predicted by HO et al. [21] and Goulden [22]:
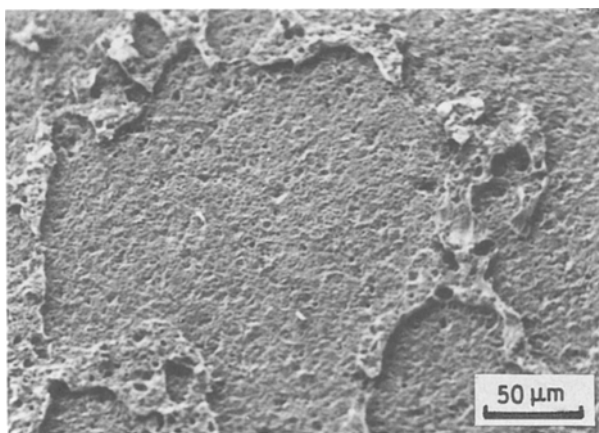
$$(0 0 1) \text{ Cu } \| \ (0 0 1) \ Cu_2O$$

or

$$(0 0 1) \text{ Cu } \| \ (1 1 1) \ Cu_2O \ [1 \ 1 \ 2] \text{ Cu } \| \ [1 \ 1 \ 0] \ Cu_2O$$

Figure 11 SEM micrograph showing the fracture surface of alumina bonded with an oxidized copper foil (oxide thickness = 0.3 μm). The adhesion area is localized around the grain boundaries of copper.
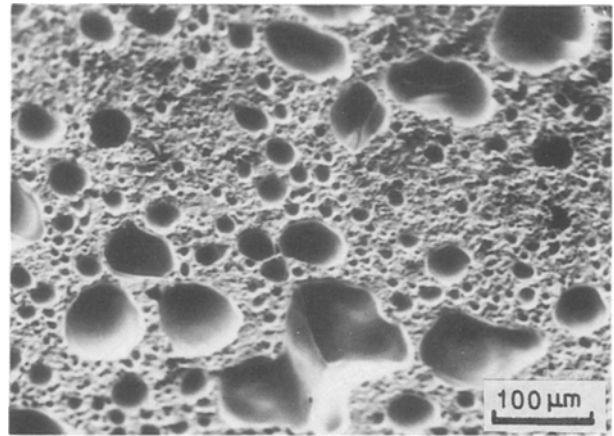

Figure 12 SEM micrograph showing pores on a copper surface strongly preoxidized (oxide thickness > 10 μm).

When increasing the bonding time (6 h), the binary oxide disappears and an alumina layer (0.2 μm thick) can be observed (Fig. 15); it has no crystallographic relationship with the bulk alumina. Small amounts of the spinel phase have been found and copper oxide is still present near by the interface (Fig. 16).

5.1.2. Reaction between Cu and Al_2O_3

In this case, no superficial oxidation of copper is performed. Before bonding, copper is treated in the same way as for mechanical characterization (vacuum annealed, 10^{-3} torr atmosphere, 1000° C for 30 min). TEM investigations show that such a reaction (2 h, 4 MPa, 1000° C, argon) leads to the formation of an alumina layer (< 0.1 μm) at the interface, unrelated to the bulk alumina (Fig. 17). The copper side is still
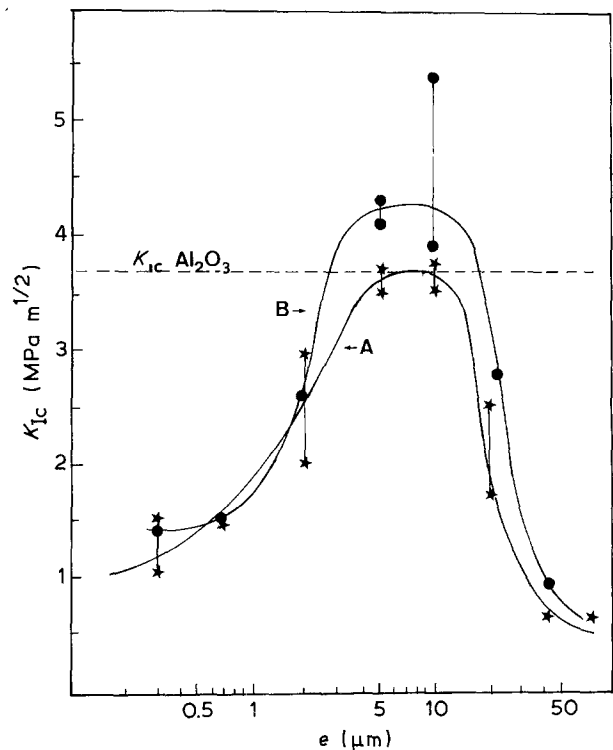

Figure 13 Fracture toughness of liquid phase bonded specimens performed on edge notched bar samples. (A) Notch located along the copper–alumina interface. (B) Notch located within the copper foil.
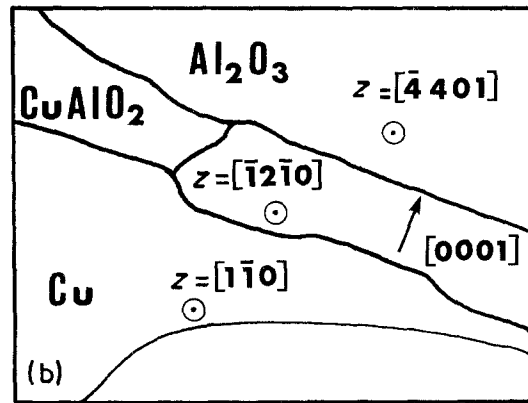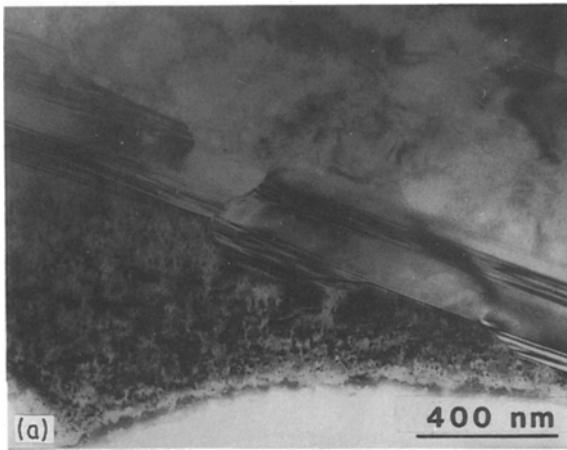
Figure 14 (a) TEM micrograph showing the presence of the binary oxide at the interface (2 h, 1000° C, 4 MPa). (b) Zone axes in the different compounds.

enriched with small precipitates of Cu_2O near by the interface.

5.2. Liquid phase reaction

In this case, the bond is strongly dependent on the wettability of the alumina surface by the liquid phase; this becomes effective when the copper oxide is entirely dissolved in the liquid phase (Fig. 18). The amount of liquid phase which is formed is proportional to the amount of copper oxide present in the system. If the thickness of the Cu_2O layer is too important, a harmful residual copper oxide layer will remain nearby the interface even when internal stresses taking off the oxide layer allow the penetration of the eutectic liquid toward the alumina surface.

The reaction between Cu_2O and alumina is fast; as shown in Fig. 19, a $CuAlO_2$ layer (0.1 μm thick) is obtained after only a few minutes of treatment. Indeed, TEM observations have never shown a Cu_2O layer, sometimes equiaxe grains (Fig. 20) are observed in opposition with the layer obtained by solid state bonding. Such grains may appear as a consequence of

the filling up of micropores or pulled out grains of alumina by the liquid phase. Moreover one can notice that the $CuAlO_2$ layer is composed of crystals whose basal planes are parallel to the interface as observed previously in solid state bonding.

The results concerning the wettability of alumina by copper–oxygen alloys (cf section 2.2) are in good agreement with the data of O'Brian and Chaklader [5]. The decrease in contact angle as oxygen content increases (related to the interfacial energy) is now explained by the presence of $CuAlO_2$ as suggested by the authors previously mentioned.

An increase in the thickness of the Cu_2O layer produces a strong drop in the mechanical properties of the bond connected with voids (Fig. 12). This may be correlated with a decomposition of the copper oxide in excess into copper and oxygen as observed by different authors [23, 24]. Oxygen in small amounts can diffuse along copper grain boundaries and precipitate.

5.3. Discussion

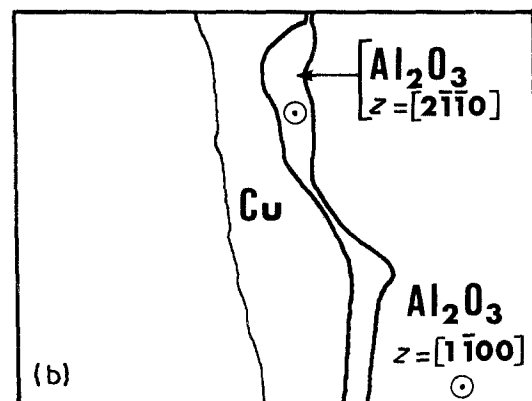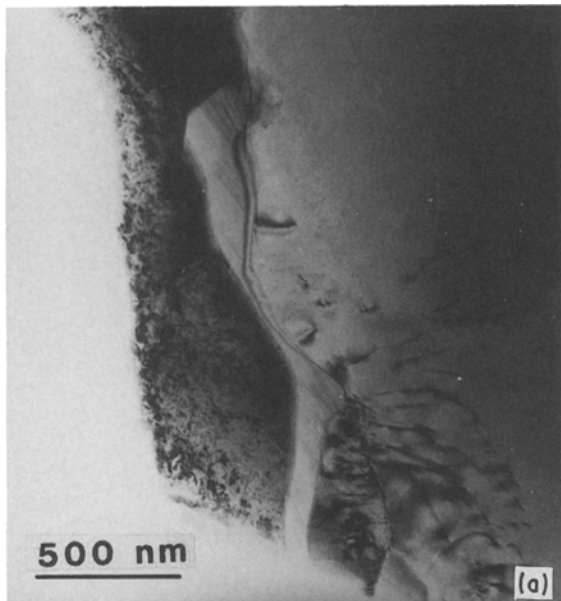The nature of the interfacial compound appears to be

Figure 15 (a) TEM micrograph showing the presence of a recrystallized alumina layer at the interface (6 h, 1000° C, 4 MPa). (b) Zone axes are shown on the diagram.
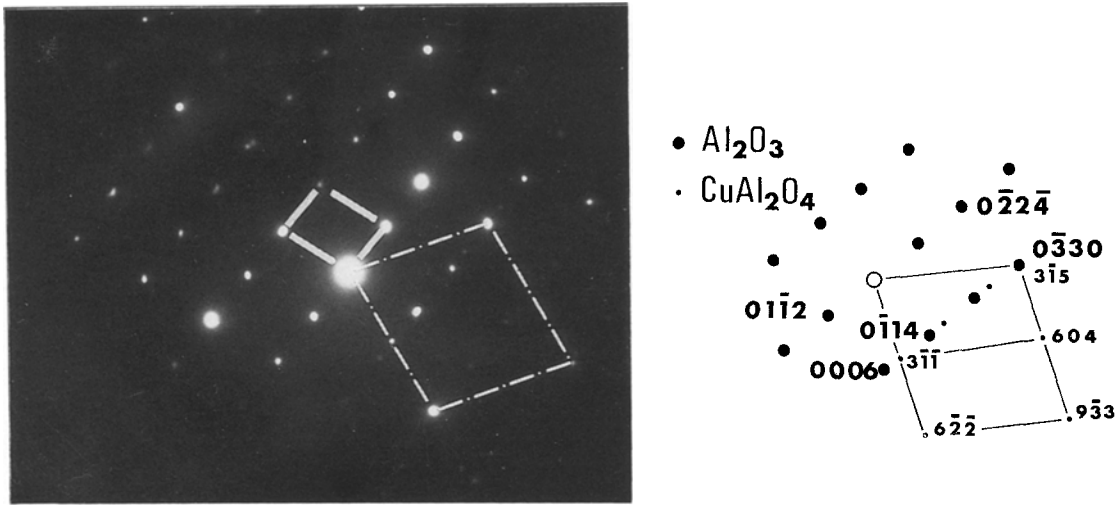
*Figure 16* Diffraction pattern obtained at the interface; diffraction spots of $CuAl_2O_4$ are indexed.

strongly dependent on the degree of oxidation of copper and on bonding time. Even when copper foils are not preoxidized, a superficial layer of copper oxide Cu_2O is still present on the copper matrix; so in any case the three components present at the interface are $Cu/Cu_2O/Al_2O_3$.

Cu_2O oxide reacts very quickly with alumina as shown by the liquid phase reaction; the $CuAlO_2$ oxide is formed in accordance with:

$$Cu_2O + Al_2O_3 \rightarrow 2\ CuAlO_2 \qquad (1)$$
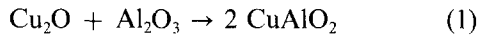
but this reaction 1 does not provide us with a detailed interfacial process.

One possibility consists in considering the decomposition of copper oxide followed by the diffusion of the Cu^+ cations toward alumina. This mechanism has already been observed during the formation of spinel oxide $ZnAl_2O_4$ as a result of a reaction between ZnO and Al_2O_3 [25]. In our case, it seems likely to consider a similar mechanism:

$$2Al_2O_3 + 3Cu^+ \rightarrow 3CuAlO_2 + Al^{3+} \qquad (2)$$

$$Al^{3+} + 2Cu_2O - 3Cu^+ \rightarrow CuAlO_2 \qquad (3)$$
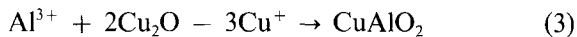
Cu^+ cations resulting from the decomposition of copper oxide diffuse toward alumina (Reaction 2), simultaneously an opposite diffusion of Al^{3+} cations occurs to react with Cu_2O and form $CuAlO_2$ (Reaction 3). On the other hand, from TEM observations one notices that the thickness of the $CuAlO_2$ layer is always less than the thickness of the initial Cu_2O layer; this brings us to consider another process which leads to the reduction of copper oxide; that is the dissolution of Cu_2O in copper by continuous diffusion of oxygen (limit of solubility: 0.036 at % at 1000° C) [26]. Such interpretation is possible considering the higher value of the diffusion coefficient for oxygen in copper: $3.1 \times 10^{-3}\ cm^2\ sec^{-1}$ in comparison with the self diffusion coefficient of copper: $1.62 \times 10^{-6}\ cm^2\ sec^{-1}$.

The oxide film acts as an oxygen source; with increasing bonding time (2 h to 6 h), the amount of Cu_2O becomes insufficient, the decrease of oxygen level gives rise to the destabilization of the less stable oxide ($CuAlO_2$) for the benefit of the oxide with the greater affinity for oxygen (alumina) (Figs 15–17) according to:
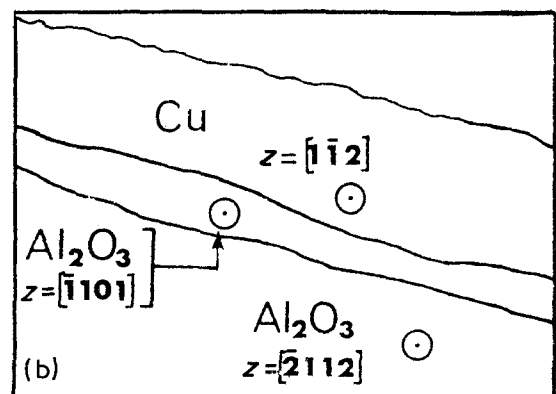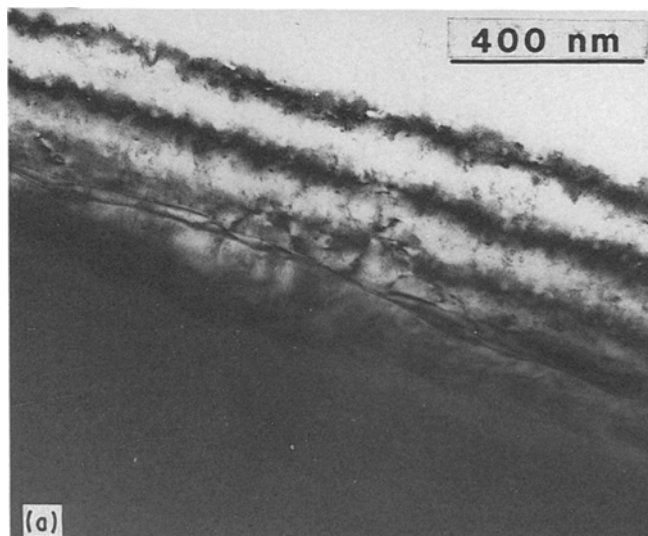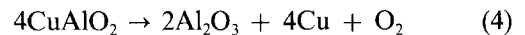
$$4CuAlO_2 \rightarrow 2Al_2O_3 + 4Cu + O_2 \qquad (4)$$

Figure 17 (a) TEM micrograph showing the presence at the interface of a small grained alumina layer ($< 0.1\ \mu m$ thick). (b) Zone axes of the different compounds are shown on the diagram.
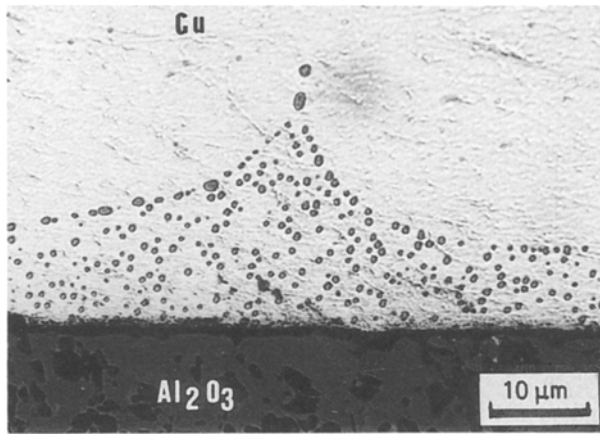
4552

Figure 18 Penetration of the eutectic liquid through the copper alumina interface (1070° C, 15 min).

The oxygen released by reaction 4 can contribute to the formation of copper oxide precipitates which are observed beneath the interface.

Anyway, we have no information concerning the diffusion coefficients of copper and aluminium in the binary oxide. It is obvious that such data should be useful interpreting experimental results.

A preliminary study by means of TEM has been carried out on $CuAlO_2$ oxide elaborated by "slurry coating" [20, 27, 28]. The $CuAlO_2$ oxide (Delafossite trigonal structure: $c/a = 5.96$) is made up [29] by an alternated stacking of atoms Cu–O–Al–O in the direction of the c-axis; the distance between the metallic planes is 0.28 nm. The value of the thermal expansion coefficient of $CuAlO_2$ along the a-axis is in good agreement with that of Al_2O_3 along the same axis.

Structural defects are present in this oxide: mainly dislocations (screw essentially) and growth twins. The mobility of these dislocations appears to be larger than in alumina [20]. Indeed, the weak beam technique has never shown a dissociation of these dislocations beyond 1.5 nm and few events have been observed
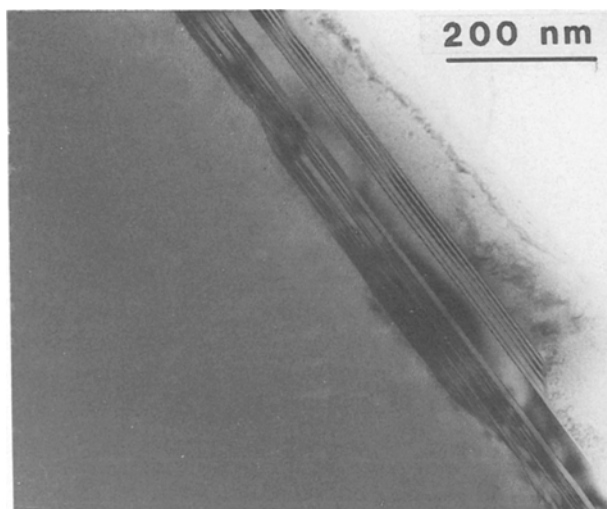

Figure 19 TEM micrograph showing the presence of the binary oxide $CuAlO_2$ at the interface. Notice (0 0 0 1) twins running parallel to the interface plane.
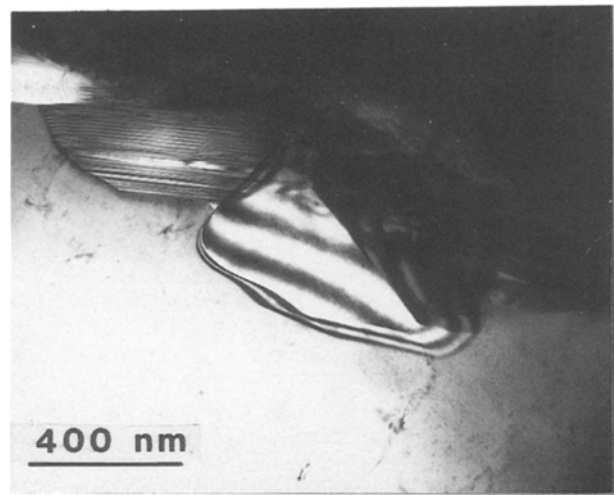

Figure 20 TEM micrograph showing $CuAlO_2$ equiaxed grains embedded in the alumina matrix.

during examination corresponding to a dislocation movement.

The glide plane is the basal plane, so in the case of $Cu–Al_2O_3$ joints this means that the $CuAlO_2$ layer has a favourable orientation for the thermal expansion accommodation due to the plasticity of this compound in the high temperature range.

One important point has to be underlined: the twinned oxide $CuAlO_2$ shows a particular orientation with the interface. The twins always present in this oxide run parallel to the basal plane and the interfacial plane, consequently these defects result from a preferential growth of the oxide along the interface which.is a nearly stress free zone. A low growth speed of the $CuAlO_2$ compound along the c-axis is understandable and can explain the decomposition of this oxide at the interface. Moreover, no particular orientation between the oxide and the interfacial plane has been detected; TEM observations performed in a direction parallel to the interface show an entanglement of $CuAlO_2$ needles.

6. Conclusion

The interaction between copper and alumina can be of a physical and physicochemical nature. The different acting phenomena are plastic deformation and metal creep, surface diffusion, evaporation–condensation in filling up the pores, surface defects and the interfacial energy. Then mechanical adhesion depends strongly on surface characteristics.

Simultaneously, chemical reactions occur between the different phases (liquid, oxides, metal) and lead to the formation of an interfacial compound ($CuAlO_2$). The extent of these redox reactions connected with the stability of the binary oxide is greatly dependent on the amount of oxygen present in the system, since it may lead to its disappearance.

Generally, a reaction layer is considered to have an undesirable effect on the bond strength. This is not true in the case of a liquid phase reaction; this process gives rise to stronger bonds than the solid phase process. This can be explained by:

1. The absence of unbonded outer areas as a

4553

consequence of a higher filling up of porosities by the liquid phase during bonding.

2. The plastic properties of the binary oxide with good capacity in accommodating the thermal deformation during cooling.

References

1. J. T. KLOMP, *Sci. Ceram.* **5** (1970) 501.
2. *Idem, Bull. Amer. Ceram. Soc.* **51** (1972) 683.
3. C. A. M. MULDER and J. T. KLOMP, *J. de Phys.* **46** (1985) 111.
4. M. TURWITT, G. ELSSNER and G. PETZOW, *ibid.* **46** (1985) 123.
5. T. E. O'BRIAN and A. C. D. CHAKLADER, *J. Amer. Ceram. Soc.* **57** (1974) 329.
6. N. EUSTATHOPOULOS and A. PASSERONE, in Proceedings of the 7th International Steelmaking Days, 1978, Versailles, France.
7. J. PASK and A. TOMSIA, in "Surfaces and Interfaces in Ceramic and Ceramic-Metal Systems", edited by J. Pask and A. Evans (Plenum, New York, 1981) p. 411.
8. G. HEIMKE and G. HEIDT, *Ber. Dt Keram. Ges.* **50** (1973) 303.
9. H. SCHMIDT-BRUCKEN and W. SCHLAPP, Keramische Zeitschrift 23 (1971) 278.
10. J. F. BURGESS, C. A. NEUGEBAUER and G. FLANAGAN, *J. Electrochem. Soc.* **122** (1975) 688.
11. M. HANSEN and K. ANDERKO, "Constitution of Binary Alloys", (McGraw Hill, New York, 1958).
12. M. COURBIERE, Thèse ECL, 1986.
13. G. HONJO, *J. Phys. Soc. Jpn* **8** (1953) 113.
14. M. COURBIERE, D. TREHEUX, C. BERAUD, C. ESNOUF, G. THOLLET and G. FANTOZZI, *J. de Phys.* **C1** (1986) 18.
15. R. F. PABST and G. ELSSNER, *J. Mater. Sci.* **15** (1980) 188.
16. J. T. KLOMP, "Science of Ceramics", edited by C. Brosset and E. Knoop (Gothenberg Swedish Institute for Silicate, 1970).
17. A. WICKER, P. DARBON and F. GRIVON, in Proceedings of International Symposium on Ceramic Compounds for Engine, Japan, 1983, p. 716.
18. S. DUSHMAN, Scientific Foundation of "Vacuum Technic" (Wiley & Son, 1962).
19. K.J. JACOB and C. B. ALCOCK, *J. Amer. Ceram. Soc.* **58** (1975) 192.
20. C. BERAUD, Thèse INSA, 1986.
21. J. H. HO and R. W. VOOK, *Phil. Mag.* **36** (1977) 1051.
22. D. A. GOULDEN, *Phil. Mag.* **33** (1976) 393.
23. I. OKAMOTO, A. OHMORI and M. KUBO, *Trans. of JWRI* **8** (1982) 123.
24. J. F. DICKSON, *Int. J. Hybrid. Micro.* **5** (1982) 103.
25. J. BENARD, in "L'oxydation des métaux", edited by Gauthier-Villars and Cie, Vol. 1, (Paris, 1962) pp. 284–285.
26. D. HANSON, C. MARRYAT and G. W. FORD, *J. Inst. Met.* **3** (1923) 197.
27. C. BERAUD, G. THOLLET, M. COURBIERE and C. ESNOUF, Colloque S.F.M.E., Strasbourg (1985).
28. M. COURBIERE, R. TRABELSI, D. TREHEUX, C. BERAUD, C. ESNOUF and G. FANTOZZI, in "High Tech Ceramics", edited by P. Vincenzini, (Elsevier, Amsterdam, 1987) pp. 2599–2608.
29. T. ISHUGURO, N. ISHIZAWA, N. MIZUTANI and M. KATO, *J. Solid State Chem.* **41** (1982) 132.